Synthesis, Characterization and Properties of (Vinyl Triethoxy Silane-grafted PP)/Silica Nanocomposites

S. Jain,[1,2] *J.G.P. Goossens,**[1,2] *M. van Duin*[3]

Summary: A new route has been developed to produce PP/silica nanocomposites starting from porous PP reactor powder and making use of sol-gel chemistry. Silica-like, nano-sized particles were prepared in the pores of the PP reactor powder with a controlled degree of adhesion between PP and silica. Magic-angle spinning (MAS) ^{29}Si NMR spectra showed that the chemical building blocks of the silica-like clusters are of Q^3 and Q^4-type. For (vinyl triethoxy silane (VTES)-grafted PP)/silica nanocomposites, VTES was grafted via solid-state modification (SSM) in porous PP particles. Subsequently, silica particles were prepared by sol-gel technology in the VTES-grafted PP. MAS ^{29}Si NMR and FT-IR spectroscopy showed that the grafted VTES becomes part of the in-situ formed silica particles. The study on the mechanical properties of (VTES-grafted PP)/silica nanocomposites showed that the silica particles improved the impact toughness of PP by a factor of 2, when there is no chemical interaction between the particles and the matrix, while for (VTES-grafted PP)/silica nanocomposites the impact toughness decreased. This indicates that chemical bonding between the filler particles and the PP-matrix results in brittle failure and supports the hypothesis that debonding is necessary for improving the impact toughness of PP with inorganic fillers.

Keywords: Crystallization; Grafting; Mechanical properties; Nanocomposites; Polypropylene

Introduction

Inorganic particle-filled polymer nanocomposites, notably (exfoliated) nano-clays, have attracted great interest over the last decade.[1–4] However, to disperse nanoparticles homogeneously in a thermoplastic via conventional melt compounding techniques is a major problem, the lack of cheap, commercially available and thermally stable organoclays and the lack of understanding of the structure/property relationships are some of the difficulties faced in the development of clay/polymer nanocomposites[5]. In the context of improving the dispersion of fillers and understanding of the structure/property relationships, it is necessary to synthesize inorganic particle-filled nanocomposites in which the interfacial strength can be tuned.

Melt compounding[6,7], solution blending[8], melt intercalation, *in-situ* intercalative polymerization[9] are well-studied methods to prepare polymer nanocomposites. Despite many efforts in the past, these conventional routes for preparing inorganic particle-filled polypropylene (PP) nanocomposites have their deficiencies and can not be exploited commercially. Moreover, during melt compounding, oxidation and β-scission lead to degradation of PP. Solvent removal is another problem faced in some of these methods. This adds extra parameters, apart from the dispersion of fillers and the interfacial strength, that

[1] Department of Chemical Engineering and Chemistry, Eindhoven University of Technology, PO Box 513, 5600 MB Eindhoven, The Netherlands
[2] Dutch Polymer Institute, PO Box 902, 5600 AX Eindhoven, The Netherlands
[3] DSM Research, PO Box 18, 6160 MD Geleen, The Netherlands

affect the morphology and the final properties of the PP nanocomposites prepared by these methods.

In view of these problems, a new strategy to prepare PP nanocomposites was developed by combining *solid-state modification* (SSM) of PP reactor powder and the *sol-gel technology* for making organic-inorganic hybrid materials[10]. SSM is a solvent-free method to modify PP largely suppressing oxidation and β-scission[11] and is advantageous due to its inherent simplicity and low temperature reaction conditions. In this study, SSM of PP involves the grafting of a polar monomer, i.e. vinyl triethoxysilane (VTES), which can subsequently be incorporated in *in-situ* made inorganic particles, thus providing chemical interaction between the matrix and the filler. An important parameter for SSM of PP is the morphology of the nascent PP powder from the polymerization reactor[12]. The porous macroparticles are composed of many sub-particles, which are also porous themselves. The PP macroparticles are approx. 300 μm and the sub-particles are in the order of 50 μm in diameter size. The irregular channels between these sub-particles are typically 2–3 μm, while the pore sizes are 2 μm at the surface to 500 nm inside the sub-particle.

Sol-gel processing is a method to produce well-dispersed, nano-scale inorganic particles in organic matrices[13–15]. The sol-gel method utilizes mild synthetic conditions, which allow versatile access to chemically designed, organo-inorganic hybrid materials and involves the hydrolysis of metal alkoxides, followed by a condensation reaction to produce metal oxides.[16]

In this paper, the solid-state grafting of VTES on PP, which enables to control the interfacial interaction between the filler and the matrix, and the subsequent *in-situ* preparation of silica-like nano-particles via the sol-gel method are discussed with the focus on the chemical and structural characterization. Further, the crystallization behavior and the mechanical properties are discussed.

Experimental

Materials

Porous, isotactic polypropylene (PP) possessing a porosity of $S_{BET\ (Kr)} = 0.0678\ m^2/g$ was supplied in powder form by EuroSabic, The Netherlands. The number-average and weight-average molecular weight of PP were 60 and 380 kg/mol respectively. The powder was free of antioxidants and stabilizers and was stored at $-10\,^{\circ}C$ in the dark. Vinyl triethoxy silane (VTES) and tetraethoxy orthosilicate (TEOS) were obtained from Aldrich Chemicals. Ammonium hydroxide (NH_4OH) (28% NH_3 in water), obtained from Aldrich Chemicals, was used as base catalyst for the sol-gel reactions. α,α'-Azoisobutyronitrile (AIBN) (Merck Schuchardt) and dibenzoyl peroxide (BPO) (Fluka Chemicals) were used as free-radical initiators.

Synthesis

All reactions were carried out in a double-skinned SSM reactor[17,18]. The reactions were carried out under a nitrogen flow to have inert atmospheric conditions and to remove traces of oxygen, which otherwise could trigger the oxidation of PP. A peristaltic pump was attached to the reactor to feed the reactant mixture at the desired rate[10]. All reactions were carried at temperatures below the melting temperature of PP. The nanocomposites and modified PP were obtained in powder form and immediately recovered from the reactor and stored at $-4\,^{\circ}C$ before further characterization.

The preparation of the (VTES-grafted PP)/silica nanocomposites was done according to the following procedure. The first step was grafting of VTES on isotactic PP via SSM. First, VTES was dispersed in the pores and subsequently migrated to the amorphous phase of PP at the reaction temperature, then the initiator was added at the desired rate. At the end of the reaction, the reactor was heated to higher temperatures to decompose all residual initiator. Subsequently, the modified PP was kept under vacuum at approx. $80\,^{\circ}C$ for

24 hrs to remove all unreacted monomers and was then stored in air-tight desiccators to avoid absorption of moisture. The second step involves the sol-gel process. TEOS was added to PP in the reactor and stirred for approx. 30 min at 60 °C. After the dispersion of TEOS, a mixture of water and ammonium hydroxide (NH_4OH) was added slowly at a controlled rate to the reactor with continuous stirring. The molar ratio of TEOS/H_2O was 1:5 and NH_4OH was 1 wt% based on TEOS. The sol-gel reaction was carried out in the reactor at 60 °C for 3 hrs with continuous stirring. The thus formed sol in PP is then gelled at 80 °C for 5 hrs and dried under vacuum at 120 °C for 24 hrs. The samples were physically mixed with antioxidants using a powder blender before any further treatment and dried under vacuum at 100 °C before chemical and structural characterization.

Fourier Transform Infrared (FT-IR) Spectroscopy

A BioRad Infrared Excalibur 3000 FTIR spectrometer was used in transmission mode to get an impression of grafting in bulk. The powder samples were melt pressed to 50 μm films at 180 °C for about 10 min using a Collin Compression Press. Melt-pressed nanocomposites were characterized in the range of 4000–400 cm^{-1} with a spectral resolution of 4 cm^{-1} and 32 scans were co-added. The calibration curve for quantitative analysis was constructed by recording FT-IR and ^1H NMR spectra of VTES-grafted PP with varying degrees of grafting. The degree of grafting (wt%) of VTES is calculated assuming that the grafted VTES is not hydrolyzed.

NMR Spectroscopy

A Varian Gemini 300 MHz NMR spectrometer was used for solution ^1H NMR to construct the calibration curve for quantitative measurements using FT-IR spectroscopy. It was also useful in determining whether the grafted monomers homopolymerize or form cross-links. Samples were prepared by dissolving grafted PP powder in deuterated tetrachloroethane, with DBPC as stabilizer, at around 140 °C, until a clear solution was obtained. All measurements for the modified PP were performed at 130 °C. In case of VTES and homopolymerized VTES, carbon tetrachloride was used as the solvent and reference, and the measurements were done at room temperature. The number of moles of grafted VTES to PP was calculated by taking the ratio of the H-atoms of the ethoxy group ($-O-CH_2-CH_3$) of VTES to that of PP.

Magic-angle-spinning (MAS) ^{29}Si NMR was carried out on a Bruker DMX500 spectrometer operating at a ^{29}Si NMR frequency of 99 MHz and equipped with a 7-mm MAS probe head and the sample rotation rate was 4 kHz (2 kHz for liquids). About 2000 scans were accumulated. MAS ^{29}Si NMR was performed to characterize the structure and the molecular connectivity of the cross-linked VTES and in-situ formed silica. A two-pulse sequence $90°$-τ-$180°$-τ was used with a $90°$ pulse of 5 μs, an echo time 2τ of 15 μs, and an interscan delay of 180 s. The peak assignments for the structure of silica is denoted by $Q^n = (RO)_{4-n}Si(OSi)_n$, as explained by Young et al.[19]. Assignments for various degrees of Si-atom substitution of the SiO_4 tetrahedra are reported elsewhere[20–22]. The peaks are located within the following range of chemical shifts relative to TMS [$Si(Me)_4$]: $Q^4 = -106$ to -120 ppm, $Q^3 = -91$ to -101 ppm, $Q^2 = -74$ to -93 ppm and $Q^1 = -68$ to -83 ppm. The chemical shift of the Si-atom next to the C=C bond in VTES is -60 ppm. It represents the T^x structure, where T^x corresponds to $Si(CH=CH_2)(OR)_{3-x}(O-Si\equiv)_x$.

Differential Scanning Calorimetry (DSC)

The crystallization and melting characteristics were investigated with a TA Instruments Q1000 Differential Scanning Calorimeter with sample weights between 3–4 mg. The analysis was conducted under standard heating and cooling rates of 10 °C/min unless otherwise indicated. Prior to the heating or cooling scan, the samples were held at 225 °C for 5 min under a nitrogen

flow to erase the thermal history and to prevent self-seeding of PP.

Mechanical Properties

Samples were prepared by first extruding the nanocomposites for homogenization and then injection molding into thick impact test bars for the impact tests. Injection molding was performed on a mini-injection molding machine (DSM). The dimensions of impact test bars were $60 \times 12 \times 4$ mm.

For high-speed impact tests, the test bars were notched with a sharp notch of 2 mm. Impact tensile tests were performed at a speed of 1 m/s, using a Zwick Rel Hydraulic testing machine. The piston displacement and force were measured at a sample rate of 2.5 MHz using a piezoelectric force transducer. The impact toughness energy was calculated by integrating the area under the measured force-displacement curves and divided by the initial cross-sectional area behind the notch. At least 5 specimens were measured and the average is reported. All the tests were performed at room temperature.

Results and Discussion

VTES Grafting on PP

The first step in the synthesis of (VTES-grafted PP)/silica nanocomposites (silica particles are in the order 20–50 nm[10]) was grafting of VTES on PP via SSM as shown in Figure 1. The free-radical initiator decomposes into free radicals, which initiate the reactions (i) by transferring the radical to the PP backbone and (ii) by addition to the monomer. Part of the monomer may homopolymerize and eventually might graft by a coupling reaction to a PP radical.

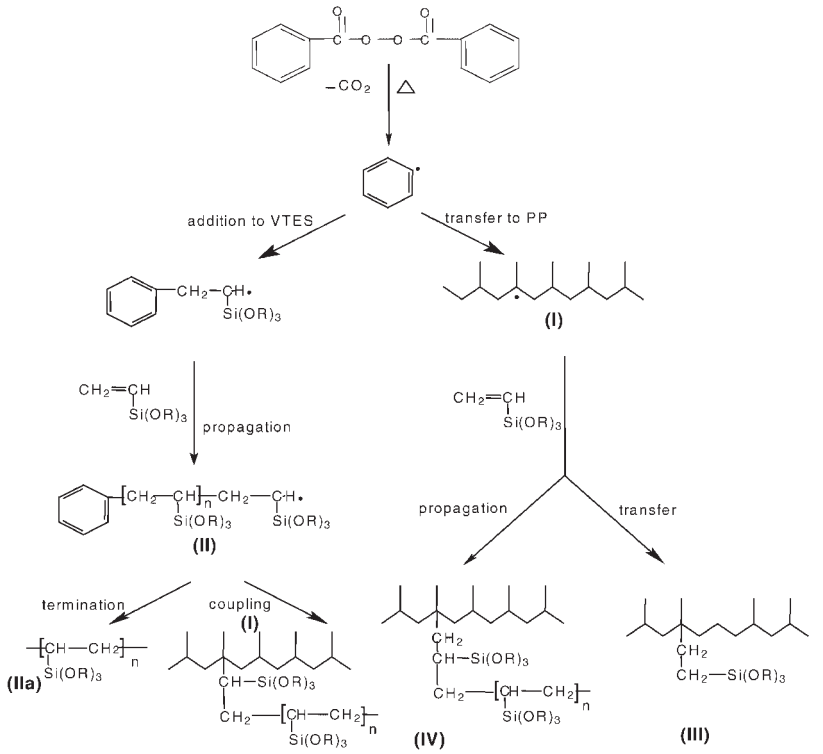

Figure 1.
Possible reactions for radical grafting of VTES on PP by initiation with peroxide during solid-state modification[10].

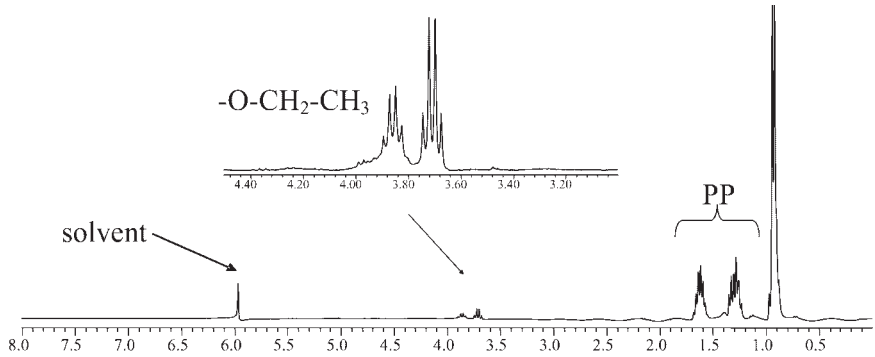

Figure 2.
^{1}H NMR spectrum of PP-*g*-VTES (13 wt%).

The structure of VTES-grafted PP was identified and the degree of grafting was quantified taking into account that VTES may homopolymerize during SSM. Figure 2 shows the ^{1}H NMR spectra of PP with 13 wt % grafted VTES. The quartet at 3.76 ppm (the inset shows the region of interest) indicates the presence of ethoxy groups attached to the Si-atom. Although no new peaks indicating the formation of aliphatic C–H groups were observed, the two quartets suggest two different structures and the broadening of the peaks indicates that VTES may have grafted as a polymer. No resonances of vinyl H-atoms were observed (~6 ppm), implying that there is no unreacted monomer in the grafted PP. The MAS ^{29}Si NMR spectra in Figure 3 of modified PP confirm the presence of grafted VTES. When VTES is attached to a long hydrocarbon chain, the ^{29}Si peak of the T^0 structure shifts to ~−45 ppm[23]. Therefore, the peak at −45 ppm in the spectrum can be assigned to VTES grafted on PP backbone. The susceptibility of VTES to homopolymerize (in bulk approx. 40% conversion with molar masses in the order of 10 kg/mol[10]), however, does not completely rule out the possibility of VTES grafting as monomer as well as polymer to PP.

The PP pores are a few micrometers in size and can act as mini-reactors inside the PP-macroparticles. The VTES can diffuse in the pores of PP or even in the amorphous phase of PP and may graft or homopolymerize there. The solubility parameter of PP is 7.43 $(cal/cc)^{1/2}$ and that of VTES is 8.0 $(cal/cc)^{1/2}$, so it is expected that the VTES can be absorbed in the amorphous phase of PP during solid-state modification. Moreover, the grafting can take place at the

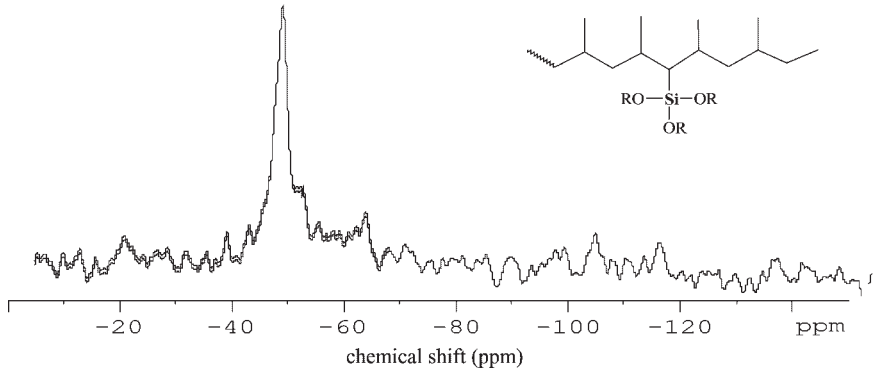

Figure 3.
MAS ^{29}Si NMR spectrum of VTES-*g*-PP monomer (10 wt%).

interface between VTES-filled pores and PP, i.e. at the PP surface. However, NMR relaxation experiments showed that grafting during SSM mainly takes place in the amorphous phase of PP. ^{1}H spin lattice relaxation times in the rotating frame, $T_{1\rho}\{H\}$, were measured for the amorphous and crystalline phase of PP via cross-polarization to ^{13}C and ^{29}Si nuclei in the solid-state. $T_{1\rho}\{H\}$ for the crystalline and amorphous phases of the original PP were found to be 35 ms and 4 ms, respectively. In case of VTES-grafted PP, it was found that $T_{1\rho}\{H\}$ for the grafted VTES was also around 4 ms, indicating that grafting took place in the amorphous phase of PP. This restricts the possibility of homopolymerization of VTES, since the diffusion of the monomer is limited by the absorption in the amorphous phase of PP and the probability that a propagating chain meets another monomer is rather small due to the 'dilution'-effect of the PP-chains.

The FT-IR spectrum in Figure 4 illustrates the grafting of VTES on PP. The strong Si–O–C stretching[24] vibration bands at 1120 cm^{-1} and 1080 cm^{-1} accompanied by a shoulder at 950 cm^{-1} are indicative for the grafting of VTES on PP. The band at ~1600 cm^{-1} corresponding to the vinyl group $CH{=}CH_2$ of VTES is absent, so no unreacted monomer is present. The cumulative area under the 1120 cm^{-1} and 1080 cm^{-1} peaks is considered to be proportional to the amount of grafted VTES. The area of the CH_3-rocking band of PP at 973 cm^{-1} was used as a reference. The overlapping of various bands in the FTIR-spectrum assigned to the CH-vibrations attached to different carbons and the similarity in the structures formed make it difficult to identify whether VTES is grafted as monomer or polymer on the PP backbone. The rapid transfer of the tertiary hydrogen abstracted from PP to the free VTES radical may prevent homopolymerization of VTES during modification of PP via SSM as explained by Rätzsch et al. for grafting of maleic anhydride in the concentration regime of interest[11]. This may suggest that VTES is grafted as a single monomeric unit on PP (*structure III* shown in Figure 1). No homopolymer of VTES was found in the pores of PP and $T_{1\rho}\{H\}$ experiments showed that VTES-containing species are present in the amorphous phase of PP as a monomeric unit on PP in the concentration range of VTES used for SSM.

Silica Synthesis in VTES-grafted PP

The FT-IR spectrum in Figure 5 shows the fingerprint of the structure of silica synthesized *in-situ* in the VTES-grafted PP. The spectra of PP/silica and (VTES-grafted PP)/silica nanocomposites show the effect of grafting on the chemical structure of silica. The peak at 1060 cm^{-1} assigned to the linear Si–O–Si linkage has shifted towards a lower wavenumber (1040 cm^{-1}) in the spectrum of (VTES-grafted PP)/silica. The peak at 1090 cm^{-1}, attributed to the

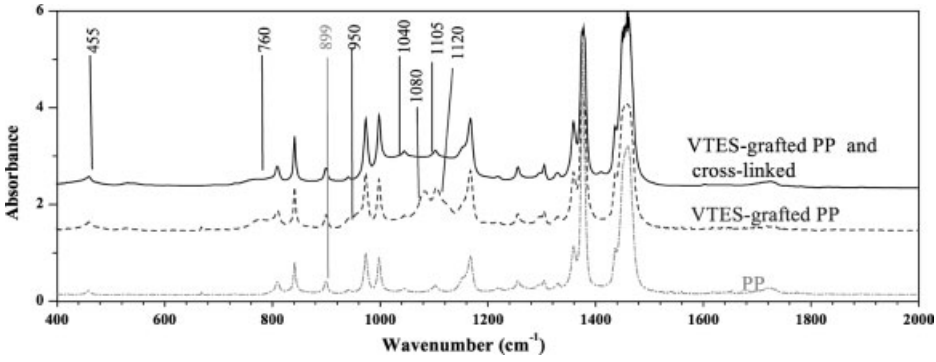

Figure 4.
FT-IR spectra of VTES-grafted PP and cross-linked VTES-grafted PP.

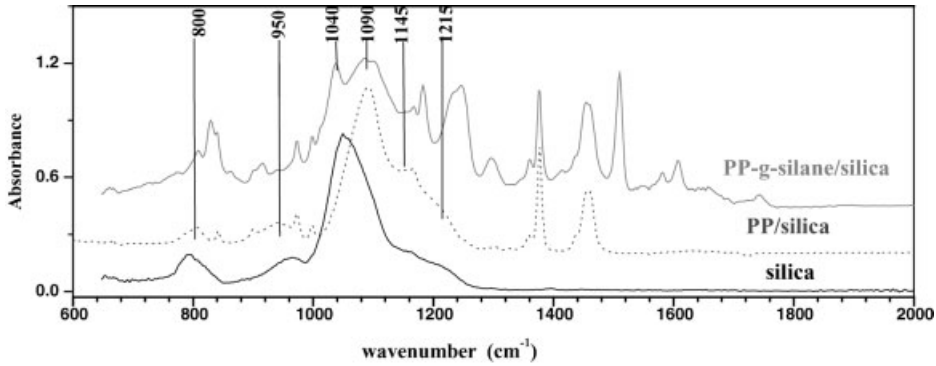

Figure 5.
FT-IR spectra of silica, and in-situ formed silica in PP and VTES-grafted PP.

Si–O–C stretching vibrations, has broadened. The broad shoulder at ~1200 cm^{-1}, assigned to the Longitudinal Optical component, is very weak. All these observations suggest that the grafted VTES takes part in the *in-situ* silica formation. There are also a number of other peaks visible which can be assigned to the phenyl-ring of the used free-radical initiator. The MAS ^{29}Si NMR spectra in Figure 6 show the structure of silica particles formed in the VTES-grafted PP. The grafted VTES (−45 ppm) converts in the presence of water and TEOS into T^0 and T^1 structures. The Q-type structures ($Q^2 \sim -92$ ppm; $Q^3 \sim -101$ ppm; $Q^4 \sim -112$ ppm) in the spectrum are assigned to the *in-situ* formed silica. From ^1H NMR, FT-IR and MAS ^{29}Si NMR, it can be inferred that grafted VTES becomes part of *in-situ* formed silica.

Crystallization Behavior of (VTES-grafted PP)/Silica Nanocomposites

The DSC cooling curves of (VTES-grafted PP)/silica nanocomposites are shown in Figure 7. The crystallization temperatures (T_c) observed for a given silica concentration show that with increasing VTES grafting T_c slightly increases. We showed that grafting of VTES alone also increases the T_c.[25] However, the increase in T_c is not high enough to be conclusive of the additional nucleating effect due to grafting of silica. The data also show that the onset of crystallization sets in at higher temperatures with increasing VTES concentration. However, the overall crystallization times are slightly longer than those of non-grafted PP/silica nanocomposites. The silica nanoparticles are attached to the PP chains through VTES and decrease the mobility and diffusivity of the polymer chains, resulting in longer times to complete the crystallization process, especially at low cooling rates. Although crystallization starts at a higher temperature due to the additional nucleating effect of VTES, the constraints on the mobility of the PP chains results in a retarded growth.

Effect of VTES Grafting on the Melting Behavior of the Nanocomposites

Figure 8 shows the melting endotherms of (VTES-grafted PP)/silica nanocomposites. An enhanced nucleation results in a higher T_c, which in turn results in more perfect and uniform crystal formation. However, due to non-random grafting multiple melting peaks can be observed. Nevertheless, the crystal size distribution is less broad compared to VTES-grafted PP via SSM. This may be due to the nucleation effect of silica nano-particles. The isothermal-crystallization behavior was investigated in various temperature regimes to get insight in the melting behavior for (VTES-grafted PP)/silica nanocomposites. Figure 9 shows the melting endotherms measured with a heating rate of 10 °C/min after isothermal crystallization at the temperature indicated above the curve. The melting behavior is similar to the observations of Lotz and

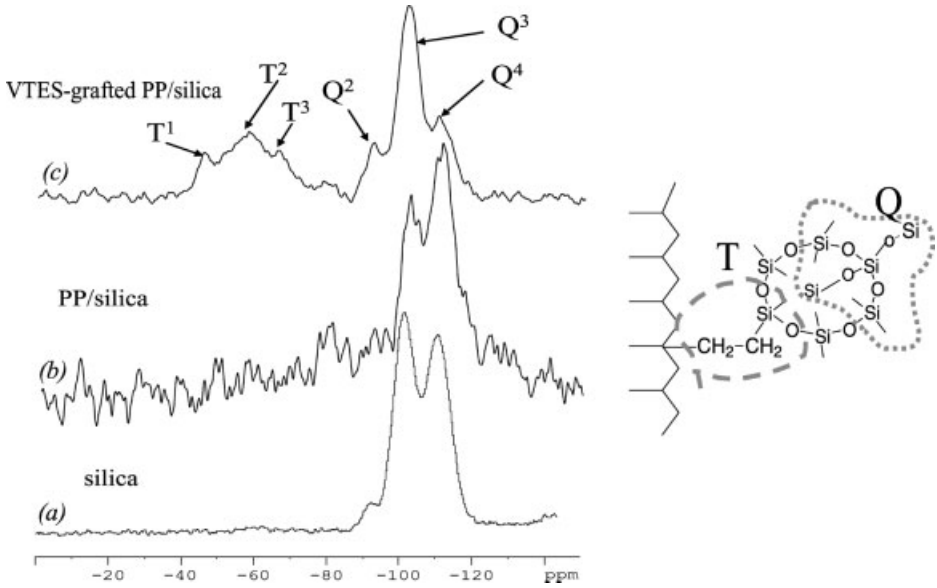

Figure 6.
MAS ^{29}Si NMR spectrum of a (VTES-grafted PP)/silica nanocomposite (the cartoon shows the T and Q-type structures).

coworkers for PP[26]. However, the temperatures at which the transitions are observed are higher than those reported by Lotz and coworkers due to the nucleating effect of silica nano-particles in VTES-grafted PP. The melting behavior itself is not so surprising, especially for PP, the details of which are reported by Varga et al.[27], who showed that if PP is cooled below a critical temperature (T^*) a considerable amount of crystals with the β-modification can be present during melting and recrystallization. The melting endotherms after isothermal crystallization at $T^* = 123\,^{\circ}C$ in this study are similar to that observed in PP when crystallized at $T^* = 105\,^{\circ}C$ by Varga et al. It shows that for (VTES-grafted PP)/silica nanocomposites, more stable β-nuclei are formed and T^* shifts to higher temperatures. The

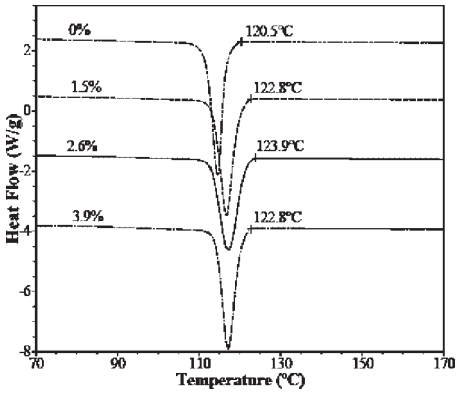

Figure 7.
The cooling exotherms of (VTES-grafted PP)/silica (the running parameter shows the percentage of VTES grafted on PP; the concentration of silica is 1 wt%).

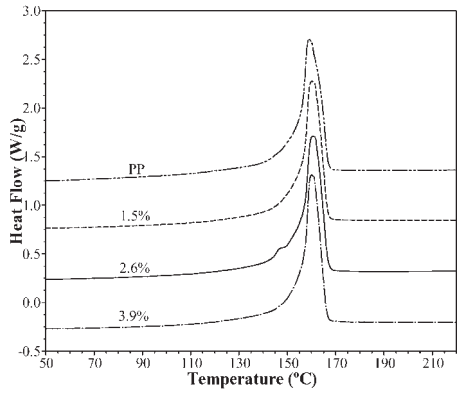

Figure 8.
Melting behavior of (VTES-grafted PP)/silica nanocomposites as a function of degree of grafting.

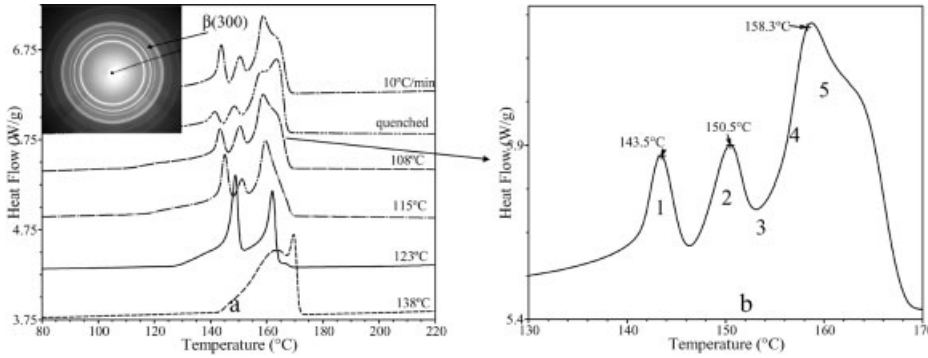

Figure 9.
(a) Melting endotherms after isothermal crystallization and 2-D WAXD pattern of VTES-grafted PP/silica nanocomposites (inset). (b) Details of multiple melting peaks: (1) melting of β-phase with partial recrystallization, (2) melting of β-phase recrystallized in the process, (3) crystallization of α-phase on $\alpha\beta^*$ latent seeds, (4) melting of α-phase, (5) melting of α-phase produced in recrystallization/melting process.

segregation of chains due to non-random grafting also helps in the early stage of crystallization. The increase in T^* also signifies that more stable α-crystals can be formed even at relatively high temperatures, and hence when (VTES-grafted PP)/silica nanocomposites are quenched, they are already in the stable crystal form compared to neat PP.

The presence of the β-modification in the quenched samples is also confirmed by the WAXD-pattern (inset in Figure 9a). This in essence shows that the β-phase formed is not an effect of the thermal treatment, but is due to the presence of silica particles.

Mechanical Properties of (VTES-grafted PP)/Silica Nanocomposites

The values of impact strength determined using high-speed tensile machine are presented in Figure 10. With addition of silica particles a two-fold increase of the impact toughness of PP can be achieved. However, (VTES-grafted PP)/silica showed no toughening effect. The impact strength of silica-filled VTES-grafted PP is similar as pure PP, but decreased compared to PP/silica. This confirms the hypothesis that a weaker interaction between rigid particles and the polymer matrix leads to a higher toughness. Similar observations were made by Thio et al.[28] in the case of glass bead-filled PP. These observations confirm the hypothesis that debonding is essential in this kind of systems.

Conclusions

(VTES-grafted PP)/silica nanocomposites were prepared by a new approach combining SSM and sol-gel technology with the idea that grafted monomeric VTES can be incorporated in the silica particles during the sol-gel reaction to control the matrix-filler adhesion. MAS ^{29}Si NMR showed that the silica clusters are predominantly Q^3 and Q^4-type, indicating that the *in-situ* formed clusters are highly condensed with some hydroxy groups at the surface. ^{1}H NMR, MAS ^{29}Si NMR and FT-IR spectroscopy studies demonstrated that VTES grafts on PP as a single monomeric unit, which is subsequently incorporated in the *in-situ* formed silica particles. SSM results in non-random grafting on VTES on PP, which affects the crystallization behavior of PP. The crystallization temperature increases with degree of grafting, indicating heterogeneous nucleation for the (VTES-grafted PP)/silica nanocomposites. The overall crystallization time is longer for the (VTES-grafted PP)/silica nanocomposites than for the PP/silica nanocomposites. The effect of covalent coupling between nano-filler to the polymer matrix on the mechan-

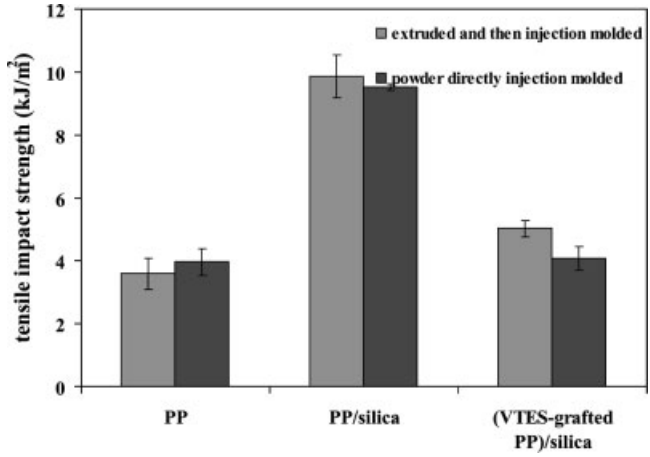

Figure 10.
High-speed tensile impact strength normalized by nominal fracture area (in all composites the concentration of silica is 2 wt% and that of grafted VTES is 2 wt%).

ical properties was evident. Silica particles improved the impact toughness of PP by a factor of 2, when there is no chemical interaction between particles and matrix. However, for the (VTES-grafted PP)/silica nanocomposites, the impact toughness decreased. This indicates that chemical bonding between filler particles and PP matrix results in brittle failure and support the hypothesis that debonding is necessary for improving the impact toughness.

[1] J. W. Gilman, C. L. Jackson, A. B. Morgan, R. Harris Jr., *Chem. Mater.* **2000**, *12*, 1866.
[2] Y. Kojima, A. Usuki, M. Kawasumi, A. Okada, Y. Fukushima, T. Kurauchi, O. Kamigaito, *J. Mater. Res.* **1993**, *8*, 1185.
[3] P. B. Messersmith, E. P. Giannelis, *J. Polym. Sci., Pol. Chem.* **1995**, *33*, 1047.
[4] R. A. Vaia, G. Price, P. N. Ruth, H. T. Nguyen, J. Lichtenhan, *Appl. Clay. Sci.* **1999**, *15*, 67.
[5] W. A. Curtin, B. W. Sheldon, *Materials Today*, **2004**, *7*, 44.
[6] M. Kato, A. Usuki, A. Okada, *J. Appl. Polym. Sci.* **1997**, *66*, 1781.
[7] A. Usuki, M. Kato, A. Okada, *J. Appl. Polym. Sci.* **1997**, *67*, 137.
[8] Y. Kurokawa, H. Yasuda, A. Oya, *J. Mater. Sci. Lett.* **1996**, *15*, 1481.
[9] S. S. Ray, M. Okamoto, *Prog. Polym. Sci.* **2003**, *28*, 1539.
[10] S. Jain, H. Goossens, F. Picchioni, P. Magusin, B. Mezari, M. van Duin, *Polymer* **2005**, *46*, 6666.
[11] M. Rätzsch, M. Arnold, E. Borsig, H. Bucka, N. Reichelt, *Prog. Polym. Sci.* **2002**, *27*, 1195.
[12] G. Cecchin, Symposium proceeding of "Polypropylene Past, Present and Future: The challenge continues"; Ferrara 19th–20th October 1998, 25.
[13] Special issue: Organic-Inorganic Nanocomposites materials *Chem. Mater.* **2001**, *13*.
[14] J. Wen, G. L. Wilkes, *Chem. Mater.* **1996**, *8*, 1667.
[15] M. W. Ellsworth, B. M. Novak, *J. Am. Chem. Soc.* **1991**, *113*, 2756.
[16] K. D. Kim, H. T. Kim, *J. Sol-gel Sci. Tech.* **2002**, *25*, 183.
[17] A. J. DeNicola, S. Guhaniyogi, *EP Patent* **1991**, EP0439079.
[18] D. Roelands, *Graduation report* **1999**, Eindhoven University of Technology, The Netherlands.
[19] S. K. Young, W. L. Jarrett, K. A. Mauritz, *Polymer* **2002**, *43*, 2311.
[20] G. Qui, Z. L. Tang, N. X. Huang, L. Gerking, *J. Appl. Polym. Sci.* **1998**, *81*, 294.
[21] E. P. Otocka, T. K. Kwei, R. Salvoey, *Macromol. Chem. Phys.* **1969**, *129*, 144.
[22] K. A. Mauritz, R. Warren, *Macromolecules* **1989**, *67*, 1799.
[23] A. Shimojima, N. Umeda, K. Kazuyuki, *Chem. Mater.* **2001**, *12*, 3610.
[24] D. A. Siuzdak, K. A. Mauritz, *J. Polym. Sci., Part B Polym. Phys.* **1999**, *37*, 143.
[25] S. Jain, *PhD-thesis* 2005, Eindhoven University of Technology, The Netherlands.
[26] B. Fillon, A. Thierry, B. Lotz, J. C. Wittman, *J. Thermal Anal.* **1994**, *42*, 721.
[27] J. Varga, *J. Thermal Analysis* **1986**, *31*, 165.
[28] Y. S. Thio, A. S. Argon, R. E. Cohen, *Polymer* **2004**, *45*, 3139.

